

# Hubbard subbands and superconductivity in the infinite-layer nickelate

Tharathep Plienbumrung,<sup>1,2</sup> Maria Daghofer,<sup>1,2</sup> Michael T. Schmid,<sup>3</sup> and Andrzej M. Oleś<sup>4,5,\*</sup>

<sup>1</sup>Institute for Functional Matter and Quantum Technologies, University of Stuttgart, Pfaffenwaldring 57, D-70550 Stuttgart, Germany

<sup>2</sup>Center for Integrated Quantum Science and Technology, University of Stuttgart, Pfaffenwaldring 57, D-70550 Stuttgart, Germany

<sup>3</sup>Waseda Research Institute for Science and Engineering, Waseda University, Okubo, Shinjuku, Tokyo, 169-8555, Japan

<sup>4</sup>Max Planck Institute for Solid State Research, Heisenbergstrasse 1, D-70569 Stuttgart, Germany

<sup>5</sup>Institute of Theoretical Physics, Jagiellonian University, Profesora Stanisława Łojasiewicza 11, PL-30348 Kraków, Poland

(Dated: November 2, 2022)

An effective two-dimensional two-band model for infinite-layer nickelates consists of bands obtained from  $d_{x^2-y^2}$  and  $s$ -like orbitals. We investigate whether it could be mapped onto a single-band Hubbard model and the filling of Hubbard bands. We find that both one-band physics and a Kondo-lattice regime emerge from the same two-orbital model, depending on the strength of electronic correlations and the filling of the itinerant  $s$ -band. Next we investigate one-particle excitations by changing the screening. First, for weak screening the strong correlations push electrons out of the  $s$ -band so that the undoped nickelate is similar to a cuprate. Second, for strong screening the  $s$  and  $d_{x^2-y^2}$  bands are both partly filled and weakly coupled. Particularly in this latter regime mapping to a one-band model gives significant spectral weight transfer between the Hubbard subbands. Finally we show how the symmetry of superconducting phases depends on the interaction parameters and determine the regions of  $d$ -wave or  $s$ -wave symmetry.

## I. INTRODUCTION

A few years ago, superconductivity was reported in infinite-layer NdNiO<sub>2</sub> thin films with Sr doping [1]. The lattice structure shares similarities with cuprate superconductors, with NiO<sub>2</sub> planes taking the place of CuO<sub>2</sub> planes. While both can be expected to be quite correlated and both show antiferromagnetic (AFM) superexchange [2–6], there are some microscopic differences. One is the lack of apical oxygens in the Ni case, which affects crystal-field energies, the other is the presence of dispersive rare-earth states close to the Fermi level. Whether one starts from isolated NiO<sub>2</sub> layers [2–8] or from band-structure calculations [9–16], one expects that more than one orbital or band might be relevant.

While single-band [17] and three-band [11, 18] models have also been proposed, two bands cross the Fermi level, see Fig. 1, and many groups have accordingly investigated two-band models [18–23]. One of the bands has a large contribution from the  $x^2 - y^2$  orbital at Ni and its dispersion is nearly perfectly two-dimensional (2D). This band can be expected to share features with the Cu-dominated band of the cuprates to be rather correlated. In the second band, rare-earth states hybridize with Ni apical states, thus obtaining some Ni( $d_{3z^2-r^2}$ ) and Ni( $d_{xy}$ ) character, however, its wave function has  $s$ -symmetry [20], and we denote it accordingly. Previous studies of various two-band models have yielded a large variety of potential pairing symmetries [7, 24], among them  $s$ ,  $d$ , and  $s_{\pm}$ -wave states [8, 11, 18], while a one-band scenario favors  $d$ -wave [17].

The  $s$ -like band lies mostly above the Fermi level, however, it forms electron pockets around the  $\Gamma$  and  $A$  points in the Brillouin zone. In the DFT band structure, the pockets account for  $\approx 7\%$  of the occupied states [25]. Even without Sr-doping, these electrons are thus missing from the  $x^2 - y^2$

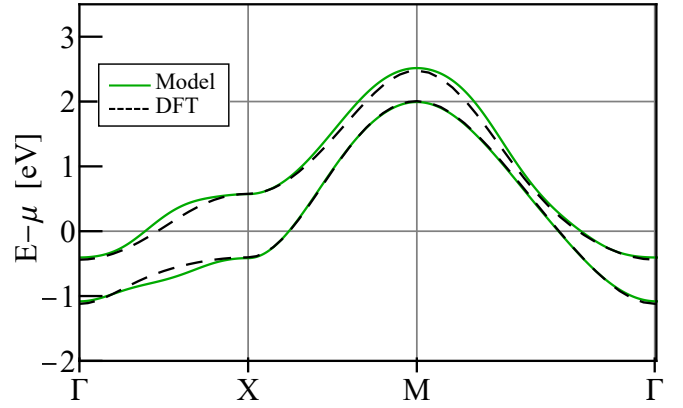


FIG. 1. Non-interacting band structure of NdNiO<sub>2</sub>: DFT bands crossing the Fermi surface (black dashed lines) and the 2D tight-binding model obtained by projecting a Wannier fit onto the plane along 2D path (green solid lines). The Fermi energy  $E = \mu$  corresponds to the DFT electronic structure.

band. When translating to a cuprate scenario, it should be noted that 5% of Sr doping suffices to destroy antiferromagnetism in La<sub>2</sub>CuO<sub>4-y</sub> [26]. We thus have to expect partly filled bands, and at least one of them is correlated.

The purpose of this paper is to investigate the evolution of the bands shown in Fig. 1 with crystal-field splittings and electron correlations in both bands. Thereby we investigate to what extent multi-band effects come into play in nickelates. It is important to realize that partial filling of the strongly correlated  $x^2 - y^2$  orbitals means that the electronic spectral weight may be transferred from the upper Hubbard band (UHB) to the lower Hubbard band (LHB) above the Fermi energy. The mechanism of such a weight transfer is well known for the doped Hubbard model [27, 28]. Another mechanism which promotes such a weight transfer is interaction screening that generates finite filling within the weakly correlated orbitals of  $s$ -wave symmetry. It is remarkable that both for

\* Corresponding author: a.m.oles@fkf.mpi.de

very weak and for strong screening the bands mostly decouple and the effective physics becomes similar to a single Hubbard band [17]. We then find a Mott insulator (doped band with potential  $d$ -wave pairing) for strong (weak) correlations. Correlation strength thus emerges as an important factor in the description of nickelate superconductors.

The remaining of this paper is organized as follows. The two-band model arises from the electronic structure calculations as described in Sec. II A. Electronic interactions are given by two Kanamori parameters for an atom  $\alpha$ :  $\{U_\alpha, J_H\}$ , and we discuss their screening in Sec. II B. Below we investigate a very wide range of potential regimes going from weak to very strong correlations in Sec. III A. There we show how the density of states changes with screening for strong and weak interactions in Sec. III B. Finally, we present the essential AFM and superconducting (SC) phases for various regimes of screening in Sec. III C. The paper is concluded in Sec. IV.

## II. TWO-BAND MODEL AND METHODS

### A. Kinetic energy

We start from the kinetic energy in the electronic structure. The DFT band structure, see Fig. 1, is calculated with QUANTUM ESPRESSO code [29–31] using a plane-wave pseudopotential method [32]. As discussed in Ref. [33], many models can be constructed that differ in the shape of the apical  $s$ -like orbital. Since their hopping integrals, given in [33], are nevertheless very similar, the kinetic energy is not affected by this ambiguity in any physically relevant way.

The Wannier90 interface [34] gives the parametrization,

$$H_{\text{kin}} = \sum_{i,\lambda=d,s;\sigma} \epsilon_\lambda d_{i\lambda\sigma}^\dagger d_{i\lambda\sigma} + \sum_{ij,\{\lambda\mu\},\sigma} t_{ij}^{\lambda\mu} d_{i\lambda\sigma}^\dagger d_{j\mu\sigma}, \quad (1)$$

where  $d_{i\lambda\sigma}$  ( $d_{i\lambda\sigma}^\dagger$ ) annihilates (creates) an electron at site  $i$  in orbital  $\lambda = d, s$ , with spin  $\sigma$ . ( $d$  and  $s$  refer to the two bands discussed above and shown in Fig. 1.) Hopping parameters  $t_{ij}^{\lambda\mu}$  and on-site energies  $\epsilon_\lambda$  are given in Ref. [33]. We project these three-dimensional bands onto the  $(x, y)$ -plane, as we are here mostly interested in the correlated  $x^2 - y^2$  states, whose band is already quite 2D to start with [33].

### B. Interactions and screening effect

While the rather extended wave-function of (especially) the  $s$ -like state might lead to longer-ranged Coulomb interactions, on-site terms can be expected to dominate and we use (intraorbital and interorbital) Coulomb elements of the form [3],

$$H_{\text{int}} = \sum_{i,\lambda=d,s} U_\lambda n_{i\lambda\uparrow} n_{i\lambda\downarrow} + \left( U' - \frac{J_H}{2} \right) \sum_i n_{id} n_{is} \quad (2) \\ - 2J_H \sum_i \vec{S}_{id} \cdot \vec{S}_{is} + J_H \sum_i \left( d_{id\uparrow}^\dagger d_{id\downarrow}^\dagger d_{is\downarrow} d_{is\uparrow} + \text{H.c.} \right).$$

$n_{i\lambda\sigma}$  is the electron number operator at site  $i$ , in orbital  $\lambda$  and for spin  $\sigma$  and  $\{\vec{S}_{i\lambda}\}$  the corresponding spin operator. Intraorbital Coulomb repulsion  $U_\lambda$  depends on the band index  $\lambda = d, s$ . Hund's exchange is given by  $J_H$  and interorbital repulsion  $U'$  couples the bands.

Upper limits for the 'bare'  $U_d$  and  $J_0$  are given by their atomic values  $U_d \approx 8$  eV and  $J_0 \approx 1.2$  eV, as one might use in modelling an insulating NiO<sub>2</sub> layer [2, 3]. However, when projecting out oxygen states and using Wannier functions instead, effective values have to be significantly reduced. In the case of  $U_s$ , atomic values for Ni cannot be even taken as a starting point, as the  $s$ -orbital is mostly made up of rare-earth states and is not centered on a Ni site [20]. The strong Nd(5d) character and very itinerant character of the  $s$ -bands suggests that their effective interaction should be strongly screened, in fact more that can be expected for the  $d$  states. One thus expects  $U_d > U_s$ , which we take into account in a phenomenological way via a screening parameter  $\alpha \in [0, 1]$ , so that

$$U_s = \alpha U_d, \quad J_H = \alpha J_0, \quad U' = U_s - 2J_H. \quad (3)$$

This parametrization provides the simplest approach to discuss the interplay of a more and a less correlated band.

We then use Lanczos exact diagonalization to treat the full Hamiltonian  $H = H_{\text{kin}} + H_{\text{int}}$  on an eight-site square cluster standing for a NiO<sub>2</sub> plane. Orbital densities are analyzed following Ref. [33] for the two orbitals,  $d$  and  $s$ . Below we summarize the evolution of the density of states in the correlated  $d$  band and the accompanying  $s$  band. We particularly focus on the circumstances favoring the electron transfer between the Hubbard subbands in the correlated band.

## III. NUMERICAL RESULTS

### A. Hubbard subbands

To understand the occurrence of possible SC phase in infinite-layer nickelates we consider first the one-particle spectra in the normal phase. Figure 2 shows the orbital-resolved density of states, taking two values of the Coulomb interaction  $U_d = 8.0$  and  $4.0$  eV. The larger value is the same as interactions in cuprates [35] and could be considered to be the upper limit; the lower value stands for effective Coulomb interactions in the metallic state in nickelates where Coulomb interactions are weaker. Here we begin with unscreened interactions in the  $s$  band, i.e., we take  $\alpha = 1.0$ .

In both cases of large  $U_d = 8.0$  eV and moderate  $U_d = 4.0$  eV, one finds a Mott insulator with two subbands separated by a gap, the occupied LHB and the empty UHB. For large  $U_d = 8.0$  eV, the gap is  $\approx 3.5$  eV and the Fermi energy falls within the gap, see Fig. 2(a). This may be considered a textbook example of a Mott insulator. Then one finds also an AFM order in the LHB.

When  $U_d = 4$  eV, the gap in the correlated band decreases to less than  $\approx 1.0$  eV and the tail of the  $s$  band falls below the Fermi energy which still separates the occupied and unoccupied states of the LHB, see Fig. 2(b). However, we should

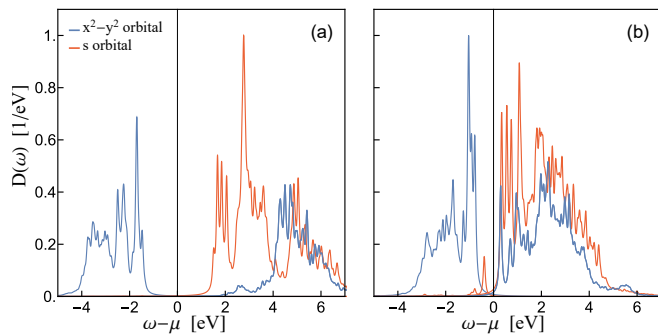


FIG. 2. Density of states  $D(\omega)$  of undoped nickelate with unscreened interactions ( $\alpha = 1$ ). Fermi energy is set to zero; the orbital densities are normalized to one (per spin). Intraorbital Coulomb interaction in Eq. (2) is selected at: (a)  $U_d = 8$  eV and (b)  $U_d = 4$  eV.

keep in mind that the calculations are done for a finite system and we cannot exclude a metallic phase in the thermodynamic limit. In any case, one finds a small fraction of electrons occupying the  $s$  states and these states are just below the Fermi energy, see Fig. 2(b). Here the correlated LHB band is less than half-filled and develops dynamics. As a result, electron transfer from the UHB to the unoccupied part of the LHB increases, and the total occupancy of the LHB exceeds 0.5. We conclude that the presence of the second more itinerant band is responsible for the electron transfer between the Hubbard subbands.

The next question to ask is where doped holes go in the quarter-filled system. Before we have shown [36] that three regimes emerge for increasing screening as discussed below. The reduction of the Coulomb interaction to  $U_d = 4.0$  eV is sufficient to cause the loss of long-range AFM order in the  $x^2 - y^2$  orbital due to reduced electron filling.

### B. One-particle spectral density

First, in the weakly screened Mott insulator and for large  $U_d$ , the ground state is AFM and holes naturally enter only the  $x^2 - y^2$  orbital. In contrast, the second regime is found at intermediate screening [ $\alpha \simeq 0.5$ ], or for interactions that are reduced from the outset, see Fig. 2(b). Finally, in the third regime of strong screening ( $\alpha \sim 0.2$ ), hole doping occurs again into the  $x^2 - y^2$  orbital, with the  $s$  electrons remaining unaffected [36]. This behaviour is presented in more detail below.

The different behaviour in the three regimes mentioned in Sec. III A is also reflected in the single-particle spectra shown in Fig. 3. Filling corresponds to doping with two holes and twisted boundary conditions (TBC) are used to resolve more momenta [37–39]. Both for very strong  $U_d = 8.0$  eV, see Fig. 3(a) and for moderate  $U_d = 4.0$  eV, see Fig. 4(a), the correlations induce a gap in the  $x^2 - y^2$  band [40]. The lowest (occupied) states for electrons are in the  $s$  band at reduced  $U_d = 4$  eV, i.e., both bands are partly filled. This can be seen in Fig. 2(b), where we show the density of states for eight electrons (i.e., at quarter filling). Data were obtained by means

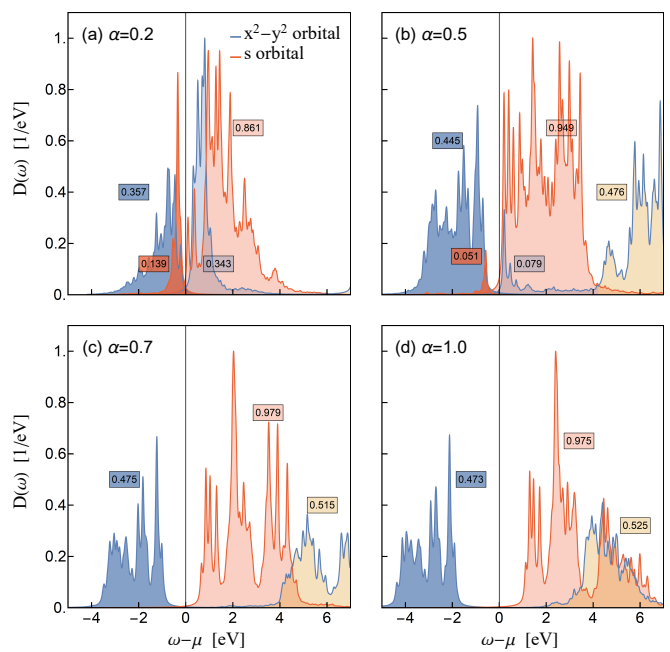


FIG. 3. Density of states  $D(\omega)$  of undoped nickelate for  $U_d = 8.0$  eV and for different values of screening  $\alpha$ .

of TBC, integrating over five sets of boundary conditions.

At strong screening when  $\alpha = 0.2$ , the occupied states in the  $x^2 - y^2$  band are rather similar for  $U_d = 8.0$  eV and  $U_d = 4.0$  eV, except that the curvature of the occupied states changes along the  $(\pi, 0) - (0, \pi)$  line. Also the values of  $n_s$  and of the weight transferred to the LHB are similar. Since

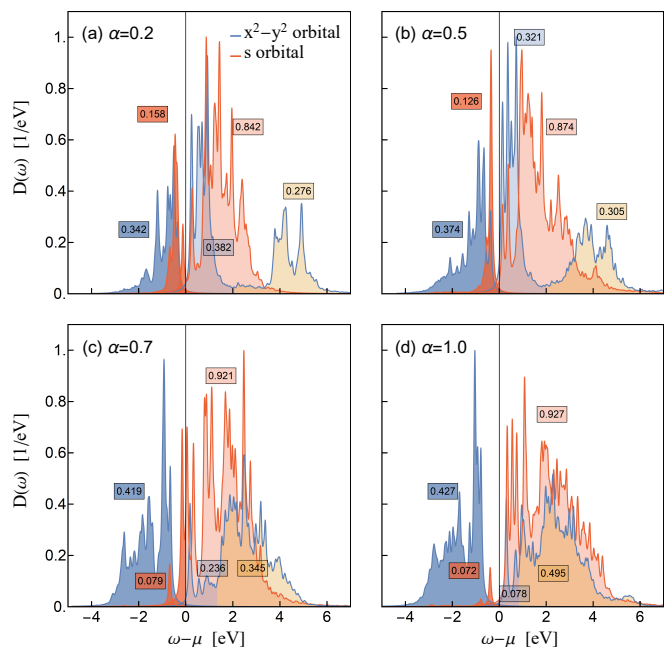


FIG. 4. Density of states  $D(\omega)$  of undoped nickelate for  $U_d = 4.0$  eV and for different values of screening  $\alpha$ .

TABLE I. Electron densities  $n_d$  and  $n_s$  per spin obtained in the undoped nickelate for screened interactions ( $\alpha < 1$ ). The weight of the LHB  $w_{\text{LHB}}$  is increased by the kinetic weight transfer from the UHB [41, 42].

$U_d$ (eV)	$\alpha$	$n_d$	$n_s$	$w_{\text{LHB}}^>$	$w_{\text{LHB}}$
8.0	0.20	0.358	0.139	0.343	0.700
	0.50	0.445	0.051	0.079	0.524
	0.70	0.475	0.021	0.011	0.485
	1.00	0.473	0.025	0.002	0.475
4.0	0.20	0.342	0.158	0.382	0.724
	0.50	0.374	0.126	0.321	0.695
	0.70	0.419	0.079	0.236	0.656
	1.00	0.427	0.072	0.078	0.505

this implies that interactions  $U'$  and  $J_H$  between  $d$  and  $s$  states do not play here a significant role, it supports the notion of a correlated (and doped)  $d$  band that is only affected by a metallic  $s$  band via self-doping.

In contrast, for stronger correlations, i.e., weaker screening  $\alpha \in [0.5, 0.7]$ , the spectra shown in Figs. 3(b) and 3(c) are affected by  $U_d$ . All electrons are here in the correlated  $x^2 - y^2$  states. It is remarkable that the occupied states fall almost at the same energies, independently of whether  $U_d = 8.0$  eV or  $U_d = 4.0$  eV [cf. Figs. 3 and 4]. However, splitting between  $d$  and  $s$  states is clearly affected by  $U_d$  (via  $U'$  and  $J_H$ ), which indicates that the  $s$ - and  $d$ -bands are in this regime directly coupled, not only via self-doping.

Analogous conclusions can be drawn from the undoped density of states shown in Figs. 3(a) and 4(a) are extremely similar: In the regime of strong screening, both bands are partly filled and results hardly depend on  $U_d$  at all. In the intermediate regime on the other hand, both bands are likewise partially filled. A comparison between Figs. 3 and 4 indicates that the  $s$  states being close to the Fermi level could be doped away. In this regime, results depend on  $U_d$ , indicating that correlations are here more important to describe low-energy features close to the Fermi level.

Interestingly, the screening increases the density of  $s$  electrons and simultaneously the density in the correlated band  $n_d$  decreases as in the undoped case the constraint  $n_d + n_s = 1$  is satisfied. This makes the LHB less than half-filled and considerable spectral weight is transferred from the UHB to the unoccupied part of the LHB (i.e., above the Fermi energy  $\mu$ ). The mechanism of such a spectral weight transfer is well known in the partly filled Hubbard model [27, 28] and explains why the weight of the LHB exceeds eventually 0.5 per spin. Here doping in the Mott insulator is mimicked by the partial filling of the  $s$  band. The largest transfer of spectral weight is found at  $U_d = 4.0$  eV and  $\alpha = 0.2$ , see Table I. The UHB forms only in the correlated  $x^2 - y^2$  band and Hubbard subbands are absent within the  $s$  band even at  $U_d = 8.0$  eV.

The regimes of weak and strong screening differ qualitatively. The number of correlated electrons  $n_d$  is close to  $n_d = 0.5$  for weak screening but decreases rapidly for large screening. As a result, the total weight in the LHB  $w_{\text{LHB}}$  increases somewhat above 0.7 both for  $U_d = 8.0$  and  $U_d = 4.0$  and the transferred weight is large, see Table I. The condi-

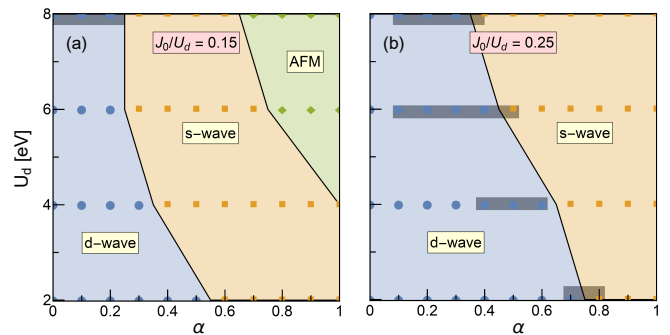


FIG. 5. Phase diagram in  $(U_d, \alpha)$  plane for increasing Hund's exchange, i.e., increasing ratio  $J_0/U_d$ : (a)  $J_0/U_d = 0.15$  (as used above); (b)  $J_0/U_d = 0.25$ . The pairing has  $s$ - and  $d$ -wave symmetry, depending on the parameters. Tendency towards triplet pairing is highlighted by gray boxes; the points mark the parameters at which the calculations were performed.

tion to activate spectral weight transfer between the Hubbard subbands is finite hole doping in the LHB of the correlated  $d$  band. Indeed, this hole doping and finite density within the  $s$  orbitals induces the spectral transfer towards the LHB in the correlated band.

Altogether, the densities of states  $D(\omega)$  give a metallic regime for intermediate ( $\alpha = 0.5$ ) and strong ( $\alpha = 0.2$ ) screening of strongly correlated  $x^2 - y^2$  states, see Fig. 3. A large gap between the Hubbard subbands opens when  $U_d = 8$  eV; this gap is reduced to  $\sim 0.5$  eV when  $U_d = 4.0$  eV. Nevertheless the system has still an insulating gap which separates the Hubbard subbands. The electronic structure for the  $x^2 - y^2$  band is typical for a doped Mott insulator, with the weight of the UHB reduced by the kinetic processes in a doped system [41, 42]. Indeed, the weight in the LHB above the Fermi energy increases by  $\sim 2\delta$  where  $\delta$  stands for the doping of the LHB, what would also be the weight transferred from the UHB to the LHB by finite doping. In this regime the  $s$  band is only weakly correlated and Hubbard subbands are poorly visible.

### C. Superconductivity in the two-band model

Finally, we investigate the nature of the SC state. Therefore, we first compute the ground state of undoped two-band model on a finite square cluster, i.e., for 8 electrons on 8-site cluster via exact (Lanczos) diagonalization. Next, the above cluster model is doped by 2 holes (by removing 2 electrons) and we look again at its ground state. After that pairing operators (for  $s$ - or  $d$ -wave) are applied on the undoped ground state and the overlap between the two states is obtained. We consider SC states of both symmetries by changing the Coulomb interaction  $U_d$  and the screening  $\alpha$  in Fig. 5.

For strong and unscreened Coulomb repulsion  $U_d > 4.0$  eV and weak Hund's exchange coupling, see Fig. 5(a), one finds AFM order in the undoped system with no sign of pairing. This regime resembles the state of cuprates: the  $s$ -like band is empty while the strongly correlated  $x^2 - y^2$  band is half-

filled and Mott insulating, see Fig. 2. This changes for weaker correlations (intermediate screening), where AFM order disappears and is replaced by  $s$ -wave pairing, see Fig. 5(b).

The presence of  $d$ -wave pairing known from cuprates requires strong screening. In the regime of strong screening doped holes enter the  $x^2 - y^2$  band and the model becomes similar to cuprate model. Altogether, Fig. 5 tells that stronger Hund's exchange promotes triplet pairing, reduces effective correlations, and suppresses AFM order.

In the phase diagram of Fig. 5(a), AFM phase and  $s$ -wave or  $d$ -wave pairings are accompanied by some indications of triplet pairing. As expected, the latter is more pronounced at stronger Hund's exchange coupling, see Fig. 5(b). Energies obtained for the doping with either one  $\uparrow$  or one  $\downarrow$  hole are here degenerate with the energies obtained with two  $\uparrow$  holes, indicating that the doped hole-pair is a triplet. In order to check the stability of this result, we used again TBC. The degeneracy is then lifted and the  $S^z = 0$  state has lower energy, suggesting that triplet pairing might be a finite-size effect. Finally, we remark that interaction screening reduces the stability of AFM order in the correlated band and broadens the range of stability of  $s$ -wave and  $d$ -wave pairings, see Fig. 5. Moreover, the needed Hund's exchange to stabilize  $d$ -wave pairing in a broad regime is rather large ( $J_0/U_d \gtrsim 0.25$ ).

#### IV. SUMMARY AND CONCLUSIONS

In summary, we have used exact diagonalization to investigate an effective two-band model for infinite-layer nickelates, where the band with a strong  $\text{Ni}(d_{x^2-y^2})$  character can be expected to be more correlated than the one with a rather extended  $s$ -like wave function of mostly rare-earth character. We focused here on the interactions in both bands, especially their relative strength, which also tunes the interorbital interactions

between the two orbitals [20]. The latter give interband interactions and could generate superconducting pairing.

We have established that both the very strongly correlated and the strongly screened regimes support the mapping of the two-band model onto a single Hubbard-like band. For (unrealistically) strong interaction  $U_d$ , we find an antiferromagnetic Mott insulator without tendencies to superconductivity. In the more realistic screened regime, the  $s$ -like band takes up some of the charge carriers and the states from both bands contribute at the Fermi energy. In this way the correlated  $x^2 - y^2$  band [17] is partly filled and the spectral weight may be transferred to the unoccupied part of the lower Hubbard band [41].

For intermediate screening the model is very rich and the  $s$ -band hosts the doped holes forming  $s$ -wave pairs. We point out that this situation broadly corresponds to a Kondo-lattice-like scenario, with the caveat that the 'localized'  $d_{x^2-y^2}$  spins can also move [4, 43, 44]. Hund's exchange coupling naturally yields ferromagnetic interaction between itinerant  $s$  carriers and  $d_{x^2-y^2}$  spins, but it is interesting to note that  $s$ -wave pairing at stronger coupling was also obtained in a similar effective model with AFM spin-spin coupling [44]. Altogether, this shows that the model investigated here is very rich and predicts pairing of different symmetry.

#### ACKNOWLEDGMENTS

We thank Wojtek Brzezicki and Andres Greco for very insightful discussions. T. Plienbunrung acknowledges Development and Promotion of Science and Technology Talents Project (DPST). A. M. Oleś acknowledges Narodowe Centrum Nauki (NCN, Poland) Project No. 2021/43/B/ST3/02166 and is grateful for support via the Alexander von Humboldt Foundation Fellowship (Humboldt-Forschungspreis).

- 
- [1] D. Li, K. Lee, B. Y. Wang, M. Osada, S. Crossley, H. R. Lee, Y. Cui, Y. Hikita, and H. Y. Hwang, Superconductivity in an infinite-layer nickelate, *Nature (London)* **572**, 624 (2019).
  - [2] M. Jiang, M. Berciu, and G. A. Sawatzky, Critical nature of the Ni spin state in doped  $\text{NdNiO}_2$ , *Phys. Rev. Lett.* **124**, 207004 (2020).
  - [3] T. Plienbunrung, M. Daghofer, and A. M. Oleś, Interplay between Zhang-Rice singlets and high-spin states in a model for doped  $\text{NiO}_2$  planes, *Phys. Rev. B* **103**, 104513 (2021).
  - [4] M. Hepting, D. Li, C. J. Jia, H. Lu, E. Paris, Y. Tseng, X. Feng, M. Osada, E. Been, Y. Hikita, Y.-D. Chuang, Z. Hussain, K. J. Zhou, A. Nag, M. Garcia-Fernandez, M. Rossi, H. Y. Huang, D. J. Huang, Z. X. Shen, T. Schmitt, H. Y. Hwang, B. Moritz, J. Zaanen, T. P. Devereaux, and W. S. Lee, Electronic structure of the parent compound of superconducting infinite-layer nickelates, *Nature Materials* **19**, 381 (2020).
  - [5] H. Lu, M. Rossi, A. Nag, M. Osada, D. F. Li, K. Lee, B. Y. Wang, M. Garcia-Fernandez, S. Agrestini, Z. X. Shen, E. M. Been, B. Moritz, T. P. Devereaux, J. Zaanen, H. Y. Hwang, K.-J. Zhou, and W. S. Lee, Magnetic excitations in infinite-layer nickelates, *Science* **373**, 213 (2021).
  - [6] J. Q. Lin, P. Villar Arribi, G. Fabbris, A. S. Botana, D. Meyers, H. Miao, Y. Shen, D. G. Mazzone, J. Feng, S. G. Chizubăian, A. Nag, A. C. Walters, M. Garcia-Fernández, K.-J. Zhou, J. Pelliciari, I. Jarrige, J. W. Freeland, J. Zhang, J. F. Mitchell, V. Bisogni, X. Liu, M. R. Norman, and M. P. M. Dean, Strong superexchange in a  $d^{9-\delta}$  nickelate revealed by resonant inelastic x-ray scattering, *Phys. Rev. Lett.* **126**, 087001 (2021).
  - [7] L.-H. Hu and C. Wu, Two-band model for magnetism and superconductivity in nickelates, *Phys. Rev. Research* **1**, 032046 (2019).
  - [8] Y.-H. Zhang and A. Vishwanath, Type-II  $t$ - $J$  model in superconducting nickelate  $\text{Nd}_{1-x}\text{Sr}_x\text{NiO}_2$ , *Phys. Rev. Research* **2**, 023112 (2020).
  - [9] P. Jiang, L. Si, Z. Liao, and Z. Zhong, Electronic structure of rare-earth infinite-layer  $R\text{NiO}_2$  ( $R=\text{La},\text{Nd}$ ), *Phys. Rev. B* **100**, 201106 (2019).
  - [10] L. Si, W. Xiao, J. Kaufmann, J. M. Tomczak, Y. Lu, Z. Zhong, and K. Held, Topotactic hydrogen in nickelate superconductors and akin infinite-layer oxides  $\text{ABO}_2$ , *Phys. Rev. Lett.* **124**, 166402 (2020).

- [11] X. Wu, D. Di Sante, T. Schwemmer, W. Hanke, H. Y. Hwang, S. Raghu, and R. Thomale, Robust  $d_{x^2-y^2}$ -wave superconductivity of infinite-layer nickelates, *Phys. Rev. B* **101**, 060504 (2020).
- [12] M. Klett, T. Schwemmer, S. Wolf, X. Wu, D. Riegler, A. Dittmaier, D. Di Sante, G. Li, W. Hanke, S. Rachel, and R. Thomale, From high  $T_c$  to low  $T_c$ : Multiorbital effects in transition metal oxides, *Phys. Rev. B* **104**, L100502 (2021).
- [13] R. Zhang, C. Lane, B. Singh, J. Nokelainen, B. Barbiellini, R. S. Markiewicz, A. Bansil, and J. Sun, Magnetic and  $f$ -electron effects in  $\text{LaNiO}_2$  and  $\text{NdNiO}_2$  nickelates with cuprate-like  $3d_{x^2-y^2}$  band, *Communications Phys.* **4**, 118 (2021).
- [14] E. Been, W.-S. Lee, H. Y. Hwang, Y. Cui, J. Zaanen, T. Devreux, B. Moritz, and C. Jia, Electronic structure trends across the rare-earth series in superconducting infinite-layer nickelates, *Phys. Rev. X* **11**, 011050 (2021).
- [15] K. Higashi, M. Winder, J. Kuneš, and A. Hariki, Core-level x-ray spectroscopy of infinite-layer nickelate: LDA + DMFT study, *Phys. Rev. X* **11**, 041009 (2021).
- [16] A. S. Botana, K.-W. Lee, M. R. Norman, V. Pardo, and W. E. Pickett, Low valence nickelates: Launching the nickel age of superconductivity, *Front. Phys.* **9**, 813532 (2021).
- [17] M. Kitatani, L. Si, R. Arita, Z. Zhong, and K. Held, Nickelate superconductors—a renaissance of the one-band Hubbard model, *npj Quantum Mat.* **5**, 59 (2020).
- [18] A. Kreisel, B. M. Andersen, A. T. Rømer, I. M. Eremin, and F. Lechermann, Superconducting instabilities in strongly correlated infinite-layer nickelates, *Phys. Rev. Lett.* **129**, 077002 (2022).
- [19] Y. Nomura, M. Hirayama, T. Tadano, Y. Yoshimoto, K. Nakamura, and R. Arita, Formation of a two-dimensional single-component correlated electron system and band engineering in the nickelate superconductor  $\text{NdNiO}_2$ , *Phys. Rev. B* **100**, 205138 (2019).
- [20] P. Adhikary, S. Bandyopadhyay, T. Das, I. Dasgupta, and T. Saha-Dasgupta, Orbital-selective superconductivity in a two-band model of infinite-layer nickelates, *Phys. Rev. B* **102**, 100501 (2020).
- [21] Y. Gu, S. Zhu, X. Wang, J. Hu, and H. Chen, A substantial hybridization between correlated Ni- $d$  orbital and itinerant electrons in infinite-layer nickelates, *Communications Physics* **3**, 84 (2020).
- [22] F. Lechermann, Multiorbital processes rule the  $\text{Nd}_{1-x}\text{Sr}_x\text{NiO}_2$  normal state, *Phys. Rev. X* **10**, 041002 (2020).
- [23] T. Y. Xie, Z. Liu, C. Cao, Z. F. Wang, J. L. Yang, and W. Zhu, Microscopic theory of superconducting phase diagram in infinite-layer nickelates, *Phys. Rev. B* **106**, 035111 (2022).
- [24] A. M. Oleś, K. Wohlfeld, and G. Khaliullin, Orbital symmetry and orbital excitations in high- $T_c$  superconductors, *Condensed Matter* **4**, 46 (2019).
- [25] A. S. Botana and M. R. Norman, Similarities and differences between  $\text{LaNiO}_2$  and  $\text{CaCuO}_2$  and implications for superconductivity, *Phys. Rev. X* **10**, 011024 (2020).
- [26] J. I. Budnick, B. Chamberland, D. P. Yang, C. Niedermayer, A. Golnik, E. Recknagel, M. Rossmannith, and A. Weidinger, Dependence of the Néel-temperatures of  $\text{La}_2\text{CuO}_4$  on Sr-doping studied by muon spin rotation, *EPL (Europhysics Letters)* **5**, 651 (1988).
- [27] H. Eskes, M. B. J. Meinders, and G. A. Sawatzky, Anomalous transfer of spectral weight in doped strongly correlated systems, *Phys. Rev. Lett.* **67**, 1035 (1991).
- [28] M. B. J. Meinders, H. Eskes, and G. A. Sawatzky, Spectral-weight transfer: Breakdown of low-energy-scale sum rules in correlated systems, *Phys. Rev. B* **48**, 3916 (1993).
- [29] P. Giannozzi, S. Baroni, N. Bonini, M. Calandra, R. Car, C. Cavazzoni, D. Ceresoli, G. L. Chiarotti, M. Cococcioni, I. Dabo, A. D. Corso, S. de Gironcoli, S. Fabris, G. Fratesi, R. Gebauer, U. Gerstmann, C. Gougousis, A. Kokalj, M. Lazzeri, L. Martin-Samos, N. Marzari, F. Mauri, R. Mazzarello, S. Paolini, A. Pasquarello, L. Paulatto, C. Sbraccia, S. Scandolo, G. Sclauzero, A. P. Seitsonen, A. Smogunov, P. Umari, and R. M. Wentzcovitch, QUANTUM ESPRESSO: a modular and open-source software project for quantum simulations of materials, *Journal of Physics: Condensed Matter* **21**, 395502 (2009).
- [30] P. Giannozzi, O. Andreussi, T. Brumme, O. Bunau, M. B. Nardelli, M. Calandra, R. Car, C. Cavazzoni, D. Ceresoli, M. Cococcioni, N. Colonna, I. Carnimeo, A. D. Corso, S. de Gironcoli, P. Delugas, R. A. DiStasio, A. Ferretti, A. Floris, G. Fratesi, G. Fugallo, R. Gebauer, U. Gerstmann, F. Giustino, T. Gorni, J. Jia, M. Kawamura, H.-Y. Ko, A. Kokalj, E. Küçükbenli, M. Lazzeri, M. Marsili, N. Marzari, F. Mauri, N. L. Nguyen, H.-V. Nguyen, A. O. de-la Roza, L. Paulatto, S. Poncé, D. Rocca, R. Sabatini, B. Santra, M. Schlipf, A. P. Seitsonen, A. Smogunov, I. Timrov, T. Thonhauser, P. Umari, N. Vast, X. Wu, and S. Baroni, Advanced capabilities for materials modelling with QUANTUM ESPRESSO, *Journal of Physics: Condensed Matter* **29**, 465901 (2017).
- [31] P. Giannozzi, O. Baseggio, P. Bonfà, D. Brunato, R. Car, I. Carnimeo, C. Cavazzoni, S. de Gironcoli, P. Delugas, F. Ferrari Ruffino, A. Ferretti, N. Marzari, I. Timrov, A. Urru, and S. Baroni, QUANTUM ESPRESSO toward the exascale, *The Journal of Chemical Physics* **152**, 154105 (2020).
- [32] A. Dal Corso, Pseudopotentials periodic table: From H to Pu, *Comp. Mat. Science* **95**, 337 (2014).
- [33] T. Plienbunrung, M. Daghofer, M. T. Schmid, and A. M. Oleś, Screening in a two-band model for superconducting infinite-layer nickelate, *Phys. Rev. B* **106**, 134504 (2022).
- [34] G. Pizzi, V. Vitale, R. Arita, S. Blügel, F. Freimuth, G. Géranton, M. Gibertini, D. Gresch, C. Johnson, T. Koretsune, J. Ibañez-Azpiroz, H. Lee, J.-M. Lihm, D. Marchand, A. Marrazzo, Y. Mokrousov, J. I. Mustafa, Y. Nohara, Y. Nomura, L. Paulatto, S. Poncé, T. Ponweiser, J. Qiao, F. Thöle, S. S. Tsirkin, M. Wierzbowska, N. Marzari, D. Vanderbilt, I. Souza, A. A. Mostofi, and J. R. Yates, Wannier90 as a community code: new features and applications, *Journal of Physics: Condensed Matter* **32**, 165902 (2020).
- [35] J. B. Grant and A. K. McMahan, Spin bags and quasiparticles in doped  $\text{La}_2\text{CuO}_4$ , *Phys. Rev. B* **46**, 8440 (1992).
- [36] T. Plienbunrung, M. T. Schmidt, M. Daghofer, and A. M. Oleś, Character of doped holes in  $\text{Nd}_{1-x}\text{Sr}_x\text{NiO}_2$ , *Condensed Matter* **6**, 33 (2021).
- [37] M. Shiroishi and M. Wadati, Integrable boundary conditions for the one-dimensional Hubbard model, *Jpn. Phys. Soc.* **66** (1997).
- [38] D. Poilblanc, Twisted boundary conditions in cluster calculations of the optical conductivity in two-dimensional lattice models, *Phys. Rev. B* **44**, 9562 (1991).
- [39] W.-G. Yin and W. Ku, Flavor-twisted boundary condition for simulations of quantum many-body systems, *Phys. Rev. B* **80**, 180402 (2009).
- [40] F. Lechermann, Late transition metal oxides with infinite-layer structure: Nickelates versus cuprates, *Phys. Rev. B* **101**, 081110 (2020).
- [41] H. Eskes and A. M. Oleś, Two Hubbard Bands: Weight Transfer in Optical and One-Particle Spectra, *Phys. Rev. Lett.* **73**, 1279 (1994).
- [42] H. Eskes, A. M. Oleś, M. B. J. Meinders, and W. Stephan, Spectral properties of the Hubbard bands, *Phys. Rev. B* **50**, 17980

- (1994).
- [43] G.-M. Zhang, Y.-F. Yang, and F.-C. Zhang, Self-doped Mott insulator for parent compounds of nickelate superconductors, *Phys. Rev. B* **101**, 020501 (2020).
- [44] Z. Wang, G.-M. Zhang, Y.-F. Yang, and F.-C. Zhang, Distinct pairing symmetries of superconductivity in infinite-layer nickelates, *Phys. Rev. B* **102**, 220501 (2020).